ORIGINAL ARTICLE

AK-GWO: a novel hybrid optimization method for accurate optimum hierarchical stiffened shells

Reza Kolahchi[1,2] · Kuo Tian[3] · Behrooz Keshtegar[4,5] · Zengcong Li[3] · Nguyen- Thoi Trung[4,5] ·
Duc-Kien Thai[6]

Abstract
The efficiency as computational efforts and accuracy as optimum design condition are two major changes in hybrid intelligent optimization methods for hierarchical stiffened shells (HSS). In this current work, a novel hybrid optimization coupled by adaptive modeling framework is proposed to improve the accuracy of the predicted optimum results of load-carrying capacity for HSS by combining active Kriging (AK) and grey wolf optimizer (AK-GWO) for optimization. In the active learning process, two data sets are introduced to train Kriging model, where active points given from initial data and adaptive points simulated based on optimal point using radial samples. The ability for accuracy of AK-GWO optimization method is compared with several soft computing models including Kriging, response surface method and support vector regression combined by GWO. The accurate results are extracted for simulating the load-carrying strength of HSS using the proposed AK-GWO method. The AK-GWO method is enhanced about 10% the accuracy of optimum load-carrying capacity with superior optimum design condition compared to other models, while the load-carrying using AK-GWO is increased about 2% compared the Kriging model.

Keywords Hybrid intelligent optimization · Adaptive learning method · Hierarchical stiffened shells · Hybrid nature-inspired method

1 Introduction

Due to high strength and stiffness of stiffened shells, these structures have widely utilized in aerospace components [1–4]. The major failure mode of stiffened shells is buckling capacity under axial compression loads [5–7]. Recently, increasing attentions on the hierarchical stiffened shell (HSS) are being paid due to its outstanding mechanical properties. In general, for robust design, the HSS is involved the multi-source dimensional uncertainties including skin, major and minor stiffeners. Wang et al. [8] first found that HSS has advantages for improving the load capacity and decreasing imperfection sensitivity. Wang et al. [9] extended HSS composed by orthogrid major and triangle minor stiffeners to improve the ability for buckling and imperfections. Advanced fabrication and failure testing investigations were carried out for the isogrid HSS and the orthogrid HSS by Li et al. [10] and Wu et al. [11]. For capturing the accurate post-buckling path, collapse point of HSS, the explicit dynamic FE framework can be used for

✉ Behrooz Keshtegar
beh.keshtegar@tdtu.edu.vn

Reza Kolahchi
rezakolahchi@duytan.edu.vn

1 Institute of Research and Development, Duy Tan University, Da Nang 550000, Vietnam

2 Faculty of Civil Engineering, Duy Tan University, Da Nang 550000, Vietnam

3 Department of Engineering Mechanics, State Key Laboratory of Structural Analysis for Industrial Equipment, Dalian University of Technology, Dalian, China

4 Division of Computational Mathematics and Engineering, Institute for Computational Science, Ton Duc Thang University, Ho Chi Minh City, Vietnam

5 Faculty of Civil Engineering, Ton Duc Thang University, Ho Chi Minh City, Vietnam

6 Department of Civil and Environmental Engineering, Sejong University, 98 Gunja-dong, Gwangjin-gu, Seoul 143-747, South Korea

the nonlinear buckling behavior as good choice due to robust analysis process with high-agreement by experimental results [12, 13]. The asymptotic homogenization method (AHM) was proposed efficient post-buckling analysis of HSSs, whose the analysis time is reduced in explicit dynamic analysis [9]. Tian et al. [14] established numerical-based smeared stiffener method (NSSM) based on AHM and Rayleigh–Ritz method, which achieves higher prediction accuracy for linear buckling load of HSSs than traditional smeared stiffener method (SSM). An adaptive strategy using NSSM was developed by Wang et al. [15] for HSSs to obtain the critical buckling mode. Tian et al. [16] proposed a fast analytical method for buckling load of shell structures using orthogonal decomposition basis eigenvalue buckling method. In the analytical approaches, the accurate result for buckling loads with fast computational time is the main changes in the robust design of HSS. Therefore, the hybrid design optimization can be used to enhance the computational burden using modelling approaches in optimization buckling capacity of HSS.

To robust design, the optimizations of HSSs are carried out for best conditions of dimensional sizes. The radial basis function (RBF) model was employed for optimizations of HSSs [15, 17, 18]. By decomposing a major (minor)-level as sub-optimization, Wang et al. [15] established a multilevel optimization method to search the global optimal solution. Tian et al. [14] proposed a competitive sampling basis surrogate model for optimizations of HSSs. the dative response surface method combined by harmony search was implemented to search the optimum conditions of stiffened panels [16]. By combining the Latinized partially stratified sampling and multi-fidelity methods, Tian et al. [19] developed enhanced variance reduction method for surrogate-based optimizations of HSSs. Recently, the variable-fidelity surrogate modelling approach for optimization HSSs was employed to improve accuracy of prediction-based surrogate model [20]. To provide the optimal results of stiffened panels, Keshtegar et al. [21] extended the adaptive harmony search combined by Kriging. Generally, the surrogate model can be combined with the optimization algorithms [22–26], for structural reliability analysis [27–33] and reliability-based design optimization [34–36]. The main effort of applied surrogate models is to provide the accurate results. However, the accurate results with efficient computation for analysis of the complex structures as HSS are the main challenge in the robust optimal design of thin-welded structures. The computation burden of HSS can be improved based on the hybrid intelligent optimization method as modelling techniques coupled by meta-heuristics optimization algorithms. However, the accurate optimal predictions using hybrid intelligent optimization method is main challenge for

approximating buckling load and mass using Kriging model to provide the reliable optimal design condition for HSS.

A novel iterative active framework procedure is proposed as hybrid intelligent optimization to extract the accurate optimal results by Kriging model. The active data and adaptive data points are used to train the Kriging models. Using optimal results of GWO, the active data are given from initial sampled data points, while the adaptive data points are randomly simulated by dynamical radial samples. The accuracy of the active Kriging is compared with several models of SVR, Kriging and RSM. The results indicated that the proposed active procedure is strongly improved the accuracy predictions of optimal results, while the safe condition is provided for optimum load capacity of HSS.

2 Analytical buckling method

2.1 Studied example of HSS

The configuration of studied HSS is displayed in Fig. 1 where diameter $D = 3000$ mm, and length $L = 2000$ mm with Young's modulus (E) of 100,000 MPa and Poisson's ratio (v) of 0.3. The HSS has nine design variables involved with continues variables (i.e., t_s = skin thickness, h_{rj} = height of major stiffener, h_{rn} = height of minor stiffener, t_{rj} = thickness of major stiffener and t_{rn} = thickness of minor stiffener) and discrete variables (i.e., N_{aj} = number of major stiffeners at axial, N_{an} = number of axial minor stiffeners between axial major stiffeners, N_{cn} = number of circumferential minor stiffeners between circumferential major stiffeners, N_{cj} = number of circumferential major stiffeners). The boundary condition is clamped at lower end and fixed at upper end. On upper end of HSS, a uniform axial load is utilized.

2.2 Analysis approach of HSS

In this paper, the explicit dynamic method is used as the analytical approach of HSS, which can capture the ultimate load-carrying capacity of HSS and yields a good agreement with the experiment [13]. The formulation of the explicit dynamic method is as follows:

$$\mathbf{Ma}_t = \mathbf{F}_t^{\text{ext}} - \mathbf{F}_t^{\text{int}} - \mathbf{CV}_t - \mathbf{KU}_t, \tag{1}$$

in which M stands mass matrix, a stands for the vector of nodal acceleration, stands for the vector of, $\mathbf{F}_t^{\text{ext}}$ and $\mathbf{F}_t^{\text{int}}$ denote applied external and internal force vector, respectively. C is damping matrix with nodal velocity vector V. K is stiffness matrix, U is nodal displacement vector,

(a) FEM   (b) Design variables
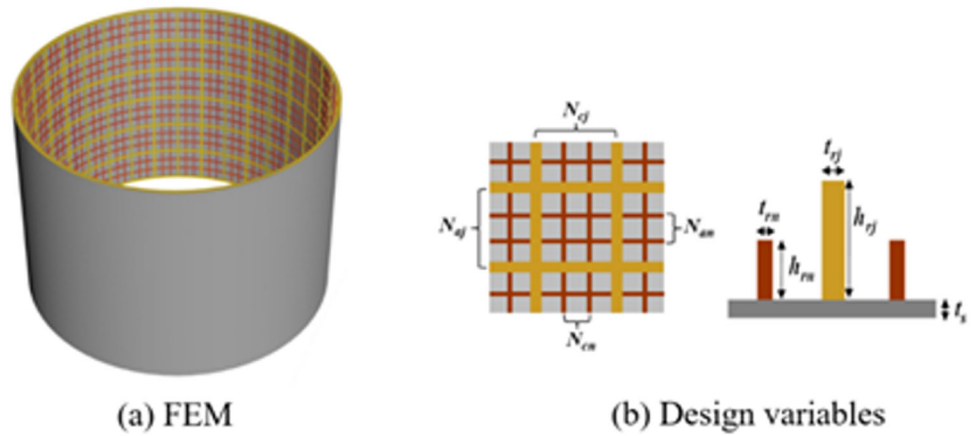
and t denotes time. Here, the central difference approach is employed to compute the explicit time integration for velocity and acceleration.

2.3 Initial database of HSS

The data points of load-carrying capacity and mass of HSS are computed based on FE method. This initial data is used for training process of the models as Kriging, SVR and RSM which are given using 400 data points. The input data for nine design variables of HSS is simulated using Latin hypercube sampling (LHS) to give the response of structures under buckling force. The input train data set and relative responses i.e., load capacity and mass of HSS which are computed by jointing nine design variables as input to a computer program. The statistical properties including maximum (X_{max}), minimum (X_{min}), average (X_{mean}), standard deviations (STD) and coefficient of variations (COV) of 400-total data for training models data are presented in Table 1. The COVs of the input variables are varied in the range from 0.2 to 0.4. As it can be seen, the load varies from 10,000 ot 35,000 kN with the mean of 18,427 kN, while mass for 200–610 kg with the mean of 351 kg. The bar diagram of the initial data points of load and mass computed by FE model is presented in Fig. 2.

Table 1 Statistical properties using 400 initial data points of design variables and FE results for load and mass

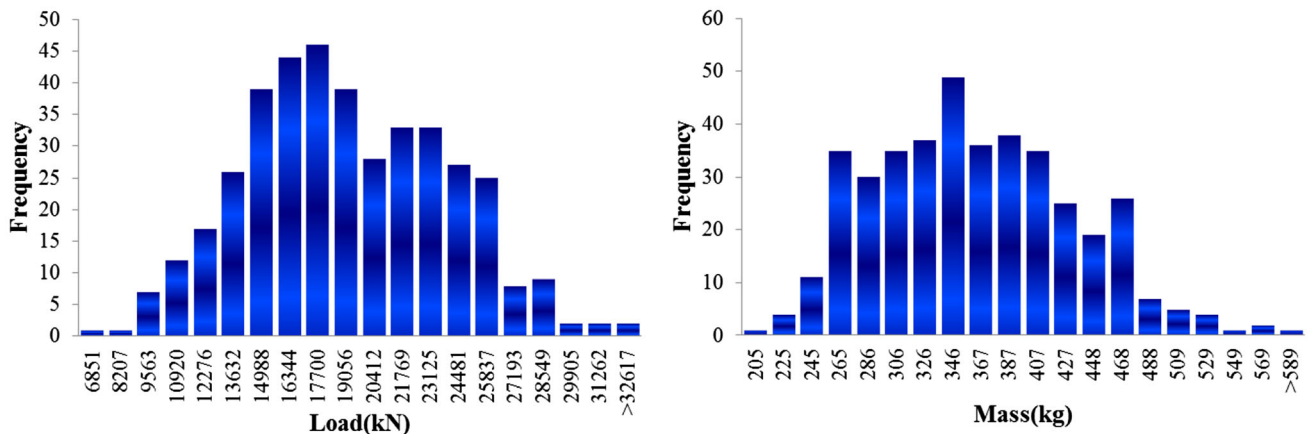| Statistics	h_{rj}	h_{rn}	N_{aj}	N_{an}	N_{cj}	N_{cn}	t_{rj}	t_{rn}	t_s	Load (kN)	Mass (kg)
X_{min}	15	9	20	1	3	1	3	3	2.5	6851.09	204.58
X_{max}	30	15	50	4	9	4	12	12	5.5	33,973.90	609.85
X_{mean}	22.5	12	35	2.5	6	2.5	7.5	7.5	4	18,427.12	351.64
STD	4.35	1.74	8.69	0.96	1.78	0.96	2.61	2.61	0.87	4829.16	71.95
COV	0.19	0.15	0.25	0.38	0.30	0.38	0.35	0.35	0.22	0.26	0.20

Fig. 2 Bar diagram of evaluated FE for load capacity and mass of HSS

3 Optimization process

In hybrid intelligent model to find design point, optimization loop is one of major importance steps. In optimization framework, the buckling load (P_{cr}) as objective function should be maximized under the mass constraint (W) as subjective function for studied HSS. The optimization model for HSS problem is described by the following optimization model:

$$\max \quad P_{cr}$$
$$\text{s.t. } W \leq 369, \tag{2}$$

where P_{cr} and W are the two approximated functions that the Kriging model used to approximate these functions based on the initial data points-based active data set and the adaptive data set in the optimization process. The input data of this problem is used to calibrate the Kriging models based on nine design variables as N_{cj}, N_{aj}, N_{cn}, N_{an}, t_s, h_{rn}, h_{rj}, t_{rj}, and t_{rn}, in which four design variables, i.e., N_{aj}, N_{cj}, N_{an}, and N_{cn} are the integer variables, while other are continues variables. The lower and upper bond of variables is, respectively, selected based on the $X_{\min}$ and $X_{\max}$, as presented in Table 1. The allowable mass in this problem is given 369 kg that it used in subjective function. Using the optimization model of HSS, the penalty strategy can be used to define the unconstraint optimization model as below:

$$\max \quad P_{cr} + \lambda \max(W - 369, 0), \tag{3}$$

where λ is the penalty factor as $\lambda = 10^4$ and $\max(W - 369, 0)$ represent the penalty function that it set to zero in the feasible domain on mass. The various optimization methods can be utilized to search optimal design of this problem [16, 22, 23, 35, 37–40]. The Grey wolf optimizer (GWO) is an swarm-inspired optimization method extracted from grey wolves in social hierarchy and hunting their behavior [41]. The GWO has advantages including solve-free mechanism, free parameters to control its convergence performance, simplicity to apply an optimization problem, and reducing the local optimum in optimization process. The presented results by [41] showed that GWO provided the highly performance to search the optimal results compared to well-known heuristics optimization algorithms. Consequently, the GWO can be used to find the optimal conditions of the complex engineering problem due to application of a random search in the optimizer processes. Recently, the GWO was implemented for optimization of different engineering problems [42, 43]. In the GWO, the random search process is obtained based on four categories of Wolf as delta (δ), beta (β), and alpha (α), while other wolves named as omega (ω). The delta (δ), beta (β), and alpha (α) are three best solutions which are used to adjust

the new position of the ω wolves. Alpha (α) Wolf has the responsibly of the optimal results among other wolves and the best solution is given based on alpha (α) Wolf, while beta (β) provides the hunting (best solution) and to give decision-making for increasing the activities of alpha (α) Wolf and reinforcing the decision of α to find best solution. Delta (δ) has the three-rank in the wolves and they provide other design domain and try for producing the best position to find the best solution for α and β wolves. The omega (ω) have the lowest ranking wolves that they control the boundaries and territory of design domain and they guarantee to safe search for find the best solution in the optimization process. The positions of δ, β, and α wolves are adjusted by the following random process using the below formulation:

$$X(t+1) = X_p(t) - A|C.X_p(t) - X(t)|, \tag{4}$$

where the position vector of wolves X is updated based on random parameter C and A at new position of $t + 1$. X_p represents the wolves position of α, β, and δ. The type of alpha provides the best optimal results among other wolf's positions. Based on the adjusting positions of the wolves, the iterative procedure to search the optimal results of HSS is given as follows:

Step 1: Define optimum model as $f(X) = P_{cr} + \lambda \max(W - 369, 0)$.

Step 2: Set the upper bound (X^U), lower bound (X^L) of design variables, numbers of wolves (NW = 10), and maximum iterations (NI = 1000).

Step 3: Uniformly initialize variables as

$$X = X^L + \text{rand}()(X^U - X^L), \tag{5}$$

where rand() is a random rand() $\in$ [0, 1] and $X \in [N_{aj}, N_{an}, N_{cn}, N_{cj}, t_s, h_{rn}, h_{rj}, t_{rj}, t_{rn}]$.

Step4: Check the boundaries of the each position for wolves as $X^L \leq X \leq X^U$.

Step 5: Compute $f(X_i)$, $i = 1, 2, \ldots,$ NW for each agent.

Step 6: Determine X_α, X_β and X_δ based on results obtained from step 5.

Step 7: Generate A and C as follows:

$$A = 2\text{rand}() \times \chi(t) - \chi(t)$$
$$C = 2\text{rand}(), \tag{6}$$

where rand() $\in [0, 1]$ and $\chi(t) = 2 - 2t/\text{NI}$. $A \in [-2, 2]$ that it is given at a small value at the final iterations, i.e., $A \sim 0$ due to $\chi(t) \sim 0$.

Step 8: determine position of each agent as below:

$$X_1 = X_\alpha - A_1|C_1.X_\alpha - X|$$
$$X_2 = X_\beta - A_2|C_2.X_\beta - X|, \tag{7}$$
$$X_3 = X_\delta - A_3|C_3.X_\delta - X|$$

where X_α, X_β and X_δ, respectively, represent the position of alpha, beta and X_δ delta wolves.

Step 9: Update the position of X X in the current solution as below:

$$X(t+1) = \frac{X_1 + X_2 + X_3}{3}. \tag{8}$$

Step 10: Control convergence as $t > \text{NI}$.

In the optimization process, the optimization function is approximated using the Kinging model. Consequently, the accurate optimal condition is directly sensitive to predictions of Kriging model to evaluate the load and mass functions. In this current work, we enhanced the predictions of Kriging–based surrogate model using an active learning procedure.

4 Active learning Kriging

The Kriging model-based data-driven is enhanced for accurate prediction of the load-capacity and mass of HSS in the optimization process. The Kriging model is trained using two active data points. In the first selected data, the initial input data points are refined by selecting the active points. In the second stage, several adaptive points are simulated in active region of optimum condition.

4.1 Kriging model

The Kriging-based surrogate model was introduced for geostatistical problems by Krige and Danie in 1952 [44] Commonly, the Kriging model-based data-driven can be implemented for approximation of the nonlinear relations in engineering problems as hydrology [45] energy of solar [16], structural design optimization [46, 47], reliability analysis [34, 48–51], reliability-based design optimization [52, 53], and etc. The Kriging model is presented as follows:

$$P(X) = g(X)^T \beta + r(X)^T \gamma. \tag{9}$$

In Kriging model, the first term, i.e., $g(X)^T \beta$ represents mathematical formulation, while the second term, i.e., $r(X)^T \gamma$ represents the stochastic relation. $g(X)$ and β, respectively, denote the basic function and unknown coefficient vectors. The stochastic term is given by Gaussian function with mean of zero and covariance vector as follows:

$$\text{cov}() = \sigma^2 R(\theta, X_p, X_q), \tag{10}$$

where σ^2 represents the variance, $R(\theta, X_p, X_q)$ denotes the correlation function between input data points X_p and X_q (p, q = 1, 2, …, m, where m is number of train data). θ in

$R(\theta, X_p, X_q)$ denotes the correlation parameter. Generally, the correlation parameter θ is computed using the following maximizing function [29, 54]:

$$L(\theta) = -m(\text{Ln}(\sigma^2) + \text{Ln}(|R|), \tag{11}$$

where Ln denotes the logarithmic operator. By determining θ, we can be given the β as below:

$$\beta = (g^T R^{-1} g)^{-1} g^T R^{-1} O, \tag{12}$$

and based on θ and β, we have

$$\gamma = R^{-1}(O - g^T \beta), \tag{13}$$

where O is observed data in train phase, R is the correlation matrix and is determined as follows [27, 28]:

$$R = \begin{bmatrix} 1 & r(X_1, X_2) & \dots & r(X_1, X_m) \\ r(X_2, X_1) & 1 & & r(X_2, X_m) \\ & \vdots & \ddots & \vdots \\ r(X_m, X_1) & r(X_m, X_1) & \cdots & 1 \end{bmatrix}, \tag{14}$$

in which $r(X_p, X_q)$ is the covariance basis function which is computed using kernel basis Gaussian function as follows [31]:

$$r(X_p, X_q) = \exp\left[-\sum_{i=1}^{k} \theta^i (X_p^i - X_q^i)^2 \right], \tag{15}$$

where θ^i, i = 1, 2, …, k represents the i-th correlation parameter for k input data. In Kriging model using the kernel function, $r(X) = [R(\theta, X_1, X), R(\theta, X_2, X), \dots, R(\theta, X_n, X)]^T$. It can be conducted that the Kriging model is predicted data using covariance term which is provide using correlation matrix R by Gaussian kernel function. Consequently, the flexibility of the Kriging model for prediction the nonlinear relation may be increased compared to the polynomial regression. The Kriging is combined with global optimization method by satisfying feasible point based on sampling set for Kriging model [23, 55]. Recently, the Kriging model was applied to optimal design condition [28]. The design domain in the optimization process is approximated based on Kriging instead of space reduction methods by expensive point strategy [38].

4.2 Active learning procedure

There is tried to increase the effect of active region of optimal design space in calibrating process of Kriging model. Therefore, an iterative regression process using Kriging approach is introduced based on two major active samples. The first samples are given from initial data presented in Sect. 2.3 for HSS, while second active points are simulated using radial random samples, which are

added into the input data set. Using the optimal design point ($X*$) given from optimization process, it is used to adjust the active and adaptive points. These data points are provided in modelling procedure as below.

4.2.1 First active data points

Using $x*$ obtained by GWO, the active points are selected from initial data points using scalar criterion which is computed as below:

$$\text{SC}_i = \|Z_i - Z^*\| \quad i = 1, 2, \ldots, \text{NS}, \tag{16}$$

where NV denotes the number of design variables. Z^* and Z_i are, respectively, the normalized design variables at optimum points ($x*$) and initial samples (x) computed as below:

$$Z_i = 2\frac{x_i - X_i^{\min}}{X_i^{\max} - X_i^{\min}} - 1 \quad -1 \leq Z_i \leq 1 \quad i = 1, 2, \ldots, \text{NV}, \tag{17}$$

in which $X_i^{\max}$ $X_i^{\min}$ are, respectively, the upper and lower bounds of ith design variable which is given based on Table 1. The active points are selected in modelling process of Kriging when $\text{SC}_i \leq \varepsilon_a$ where, ε_a is a factor.

4.2.2 Adaptive data points

In the proposed active model, several additive points are randomly simulated to increase the data set at the optimal region. Using optimal design point (Z^*), the normalized adaptive random points are generated as follows:

$$Z_{Ai} = R \times \text{rand}() \times \exp(-k)\frac{\text{RD}_i}{\|\text{RD}_i\|} + Z^* \tag{18}$$
$$i = 1, 2, \ldots, \text{NA},$$

where R is the control factor, i.e., $0.1 \leq R \leq 1$, k is iteration number to provide the additive points. $\text{rand}() \in [0, 1]$. RD_i is the random input point. The adaptive points are generated using random radius of $R \times \text{rand}() \times \exp(-k)\frac{\text{RD}_i}{\|\text{RD}_i\|}$. By increasing the iteration number to build the Kriging model in the optimization process, the random radius is decreased to provide. This means that, the additive data samples are located on the optimal design domain. Consequently, the predictions of Kinging model may be improved to evaluate the accurate results of optimal conditions for HSS. In this current work, we used $R = 0.5$.

4.3 Framework of AK-GWO

Using additive and active points, the surrogate model is regressed then; calibrated model is implemented for approximating the optimum model of HSS in GWO

framework presented in Fig. 3. In the first iteration, The Kriging model is trained using initial data. However, the Kriging model is adapted by the active process. The input dataset applied to train Kriging model are presented as below steps:

Step 1: Give the optimum point ($x*$), number of adaptive points (NA), R and the iterations for training the Kriging model (k).

Step 2: Normalize input data (Z_i).

Step 3: Select the active data as $Z_{ai} \in \{Z_i | \text{SC}_i \leq \varepsilon_a \ i = 1, 2, \ldots, \text{NS}\}$.

Step 4: Generate RD = rand(NA, NV).

Step 5: Create the adaptive points using Eq. (18)

Step 6: Transfer active and adaptive data into original space as below:

$$x_i = \frac{Z_i + 1}{2}(X_i^{\max} - X_i^{\min}) + X_i^{\min}. \tag{19}$$

Step 7: Compute the buckling loads and mass of HSS for adaptive points.

The optimization result is affected on the active and adaptive points due to applying the optimal point. The framework of hybrid intelligent optimization method is proposed in the Fig. 3. The final optimal result is given as solution when the new optimum design point is followed on the previous optimum point. In this framework, the GWO is used to search the optimal conditions, while Kriging model is actively learned using adaptive and active points. The adaptive data is jointed to the FE model to give the buckling load and mass. The proposed hybrid modelling and nature-inspired optimization method involves two major loops as optimization operated by GWO and modelling loop operated using Kriging model trained by the active data sets.

5 Results and discussion

The abilities of proposed method for accurate optimum results are compared with Kriging without active learning process, response surface method and support vector regression. The parameter of the SVR are given as $C = 9000$, $\sigma = 16.5$ and $\varepsilon = 0.25$ in training phase buckling load and $C = 5000$, $\sigma = 15$ and $\varepsilon = 0.15$ in training process of mass. The factors to active learning Kriging model are set as $\varepsilon_a = R = 0.5$ and $\|Z^*(k) - Z^*(k - 1)\| < 10^{-2}$ is used for stopping criterion of the proposed hybrid intelligent model.

The results of the hybrid intelligent model as active Kriging combined by GWO are presented in Table 2. However, the relative buckling modes corresponding to each iterations 1–6 of active learning Kriging for studied HSS are presented in Fig. 4. By comparing results in Table 2 and Fig. 4, it can be conducted that the different
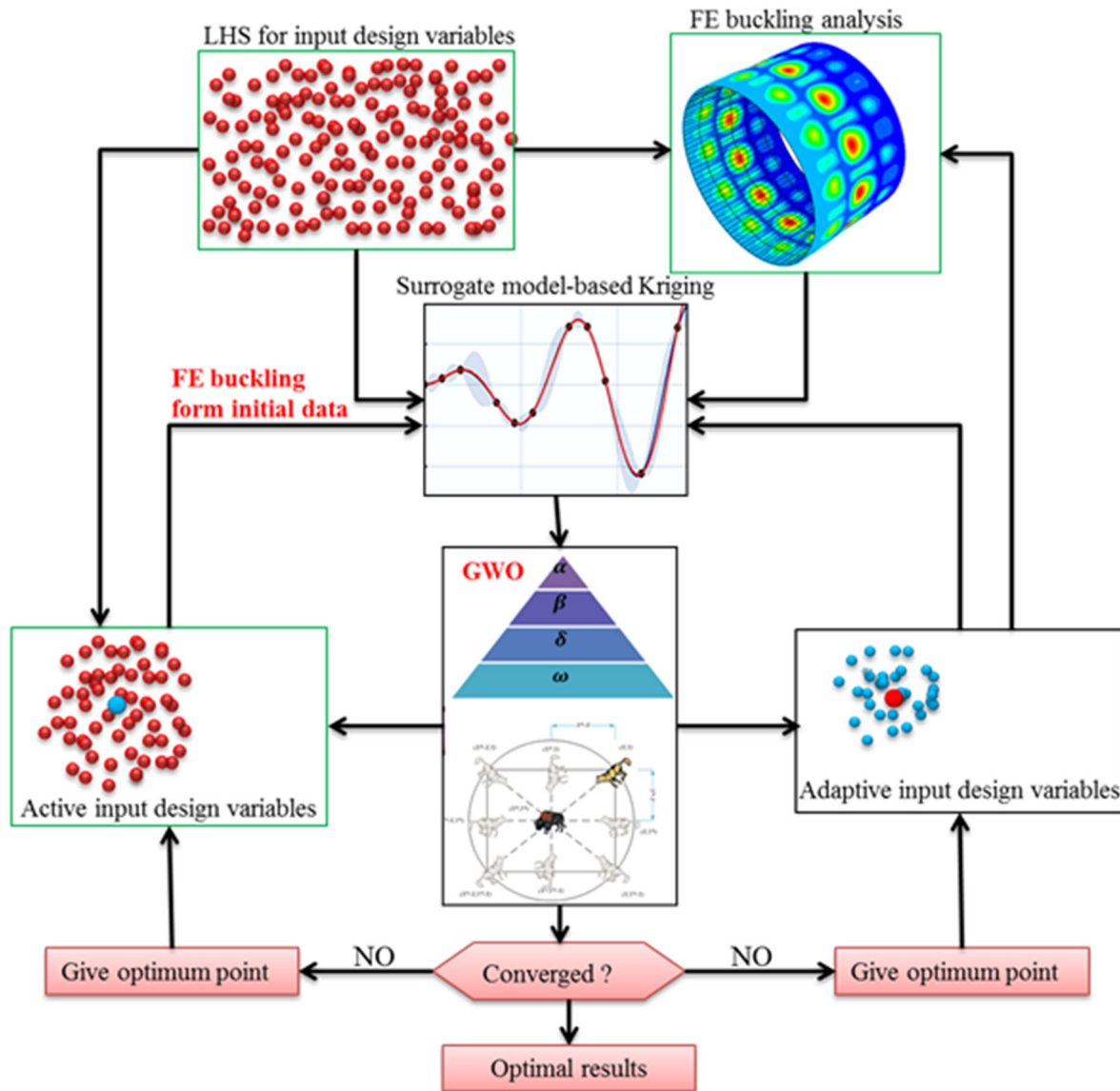
Fig. 3 Framework of proposed intelligent optimization method for HSS

predictions for loads are obtained in the first and second iterations. This means that the active data to increase the optimal domain in the optimization process may be improve the prediction of the buckling load. On the other hand at the final iterations, the buckling load predictions are followed to the same results as 23,330 kN.

Buckling modes for different iterations at optimum point of hybrid intelligent method for HSS are plotted in Fig. 4. It can be observed that, these buckling modes are all global buckling modes, which are considered as buckling modes with high load-carrying capacity for HSS [14].

The iterative procedure-based Step 1 to Step 6 of the active data points from initial simulation and adaptive data points from radial sampling for studied method are showed in Fig. 5 based on two principal dimensions which is

computed based on principal component analysis (PCA) [56]. Note from Fig. 5 that the adaptive points are increased the chance to simulate the optimal design domain, while the active point is selected form initial database. By comparing the results, it can be conducted that the active data and adaptive data points of Step 5 are similar to Step 6.

Figure 6 illustrates the obtained results from the intelligent approach using AK and the FE model at the optimal design points for load and mass of HSS. It can be conducted that the accuracy prediction of Kriging for mass is more than the buckling load, while the approximated buckling loads by active learning Kriging model are followed to the FE results as well as the mass at the final iteration. This means that the proposed stagey can be
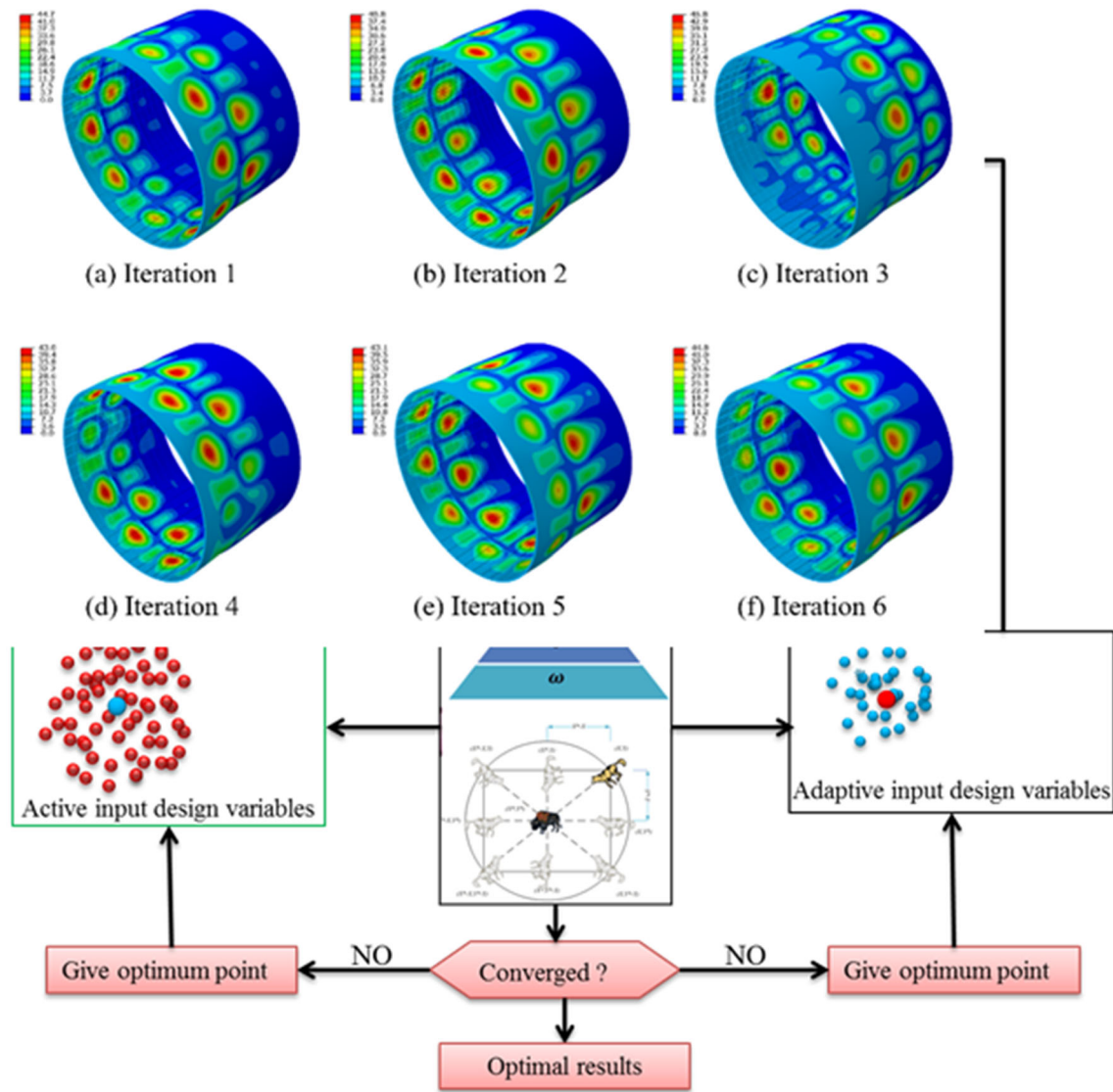
Fig. 4 Buckling mode at the optimum design point for different iterations of hybrid intelligent method for HSS

Table 2 Iterative results of the proposed hybrid intelligent method for HSS structure

Iteration	h_{rj}	h_{rn}	N_{aj}	N_{an}	N_{cj}	N_{cn}	t_{rj}	t_{rn}	t_s	Load (kN)	Mass (kg)
1	30	15	50	3	3	4	3	3	5.305	25,188.54	369.00
2	30	15	48	2	3	4	3	5.048	5.057	23,878.47	368.99
3	29.916	13.5715	50	3	3	4	3	3	5.5	23,644.04	369.00
4	30	15	50	3	3	3	3	3.493	5.218	23,167.56	369.00
5	30	15	48	3	3	2	3	3.948	5.264	23,391.24	369.000
6	29.954	14.7329	48	3	3	2	3.002	4.409	5.179	23,329.24	369.00

provided the accurate results compared the Kriging combined by GWO.

The optimal design for different models as Kriging, AK-Kriging, SVR and RSM are presented in Table 3. As seen from the results of Table 3, the AK- Kriging is improved the accuracy of the Kriging model for load about 10% from 25,188.54 to 23,329.24 kN and for mass about 0.6% from 366.60 to 368.94 kg. By comparing the FE results for all models, the Kriging and AK-Kriging are satisfied the mass constraint of the optimum model for HSS as $W \leq 369$. Whereas, SVR and RSM models are provided optimal mass more than the 369 kg. Therefore, it can be conducted
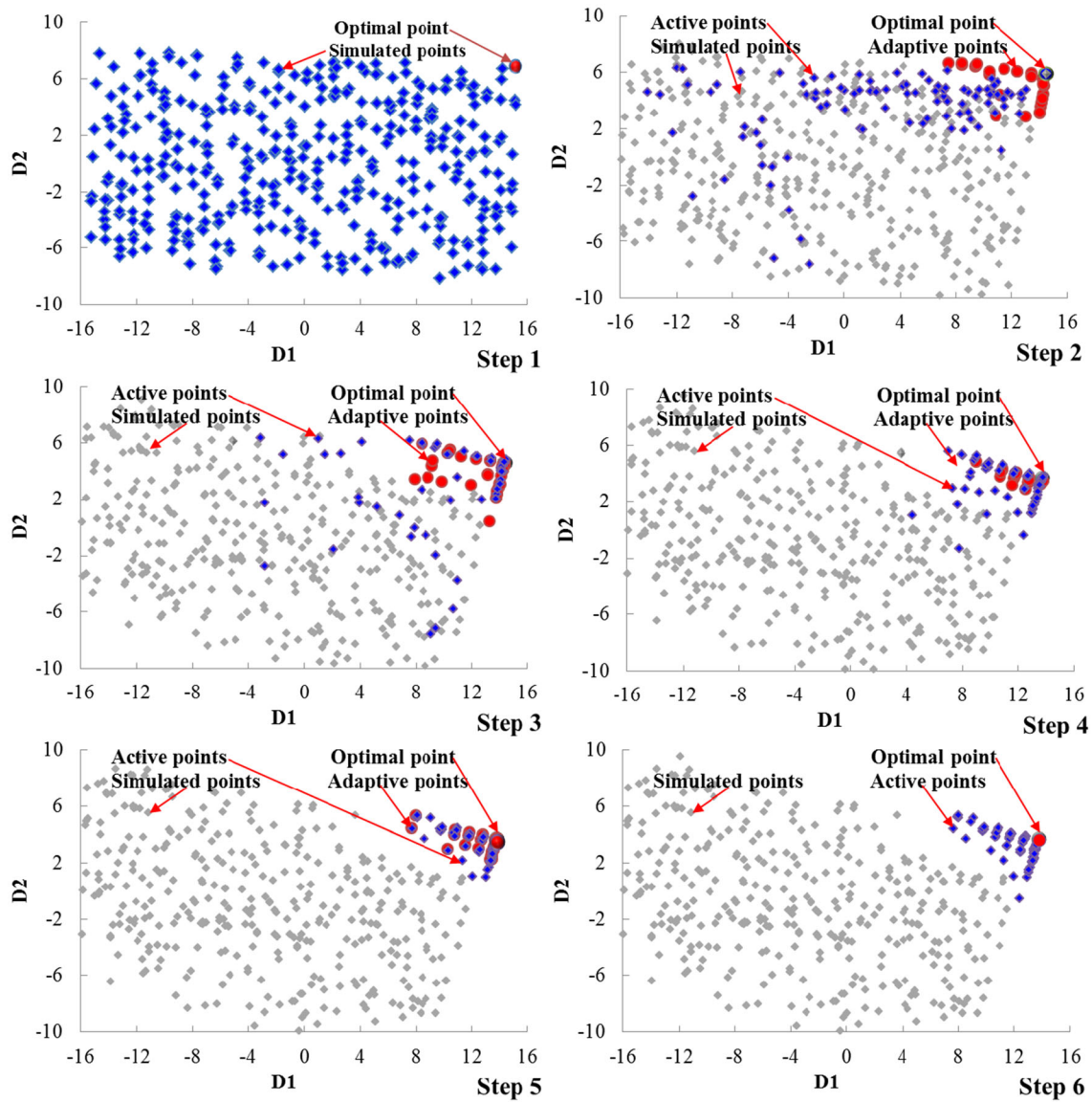
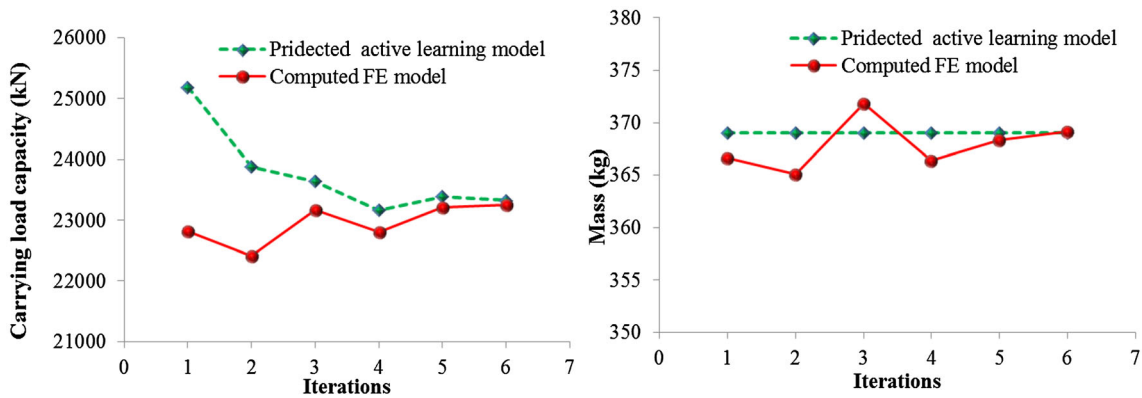**Fig. 5** Two-dimensional reduction of simulating input data using PCA for HSS

Fig. 6 Comparative results of load and mass using active learning Kriging and FE models

Table 3 Comparative optimal results for different models in studied HSS

Method	Kriging	AK-Kriging	SVR	RSM
Optimal design point				
h_{rj}	30	29.954	30	30
h_{rn}	15	14.733	14.99	15
N_{aj}	50	48	39	33
N_{an}	3	3	4	4
N_{cj}	3	3	4	3
N_{cn}	4	2	1	1
t_{rj}	3	3.002	4.399	3
t_{rn}	3	4.409	3	10.158
t_s	5.305	5.179	5.553	4.33
Predicted results				
Load (kN)	25,188.54	23,329.24	23,764.18	23,383.90
Mass (kg)	369.00	369.00	369.00	369.00
FE results				
Load (kN)	22,817.85	23,252.35	24,023.45	23,906.05
Mass (kg)	366.60	368.94	383.14	379.22
Relative error				
Load (%)	10.39	0.33	1.08	2.18
Mass (%)	0.66	0.02	3.69	2.70

Fig. 7 Comparing the buckling mode at optimum design point for different models for HSS

(a) Kriging

(b) AK-Kriging

(c) SVR

(d) RSM
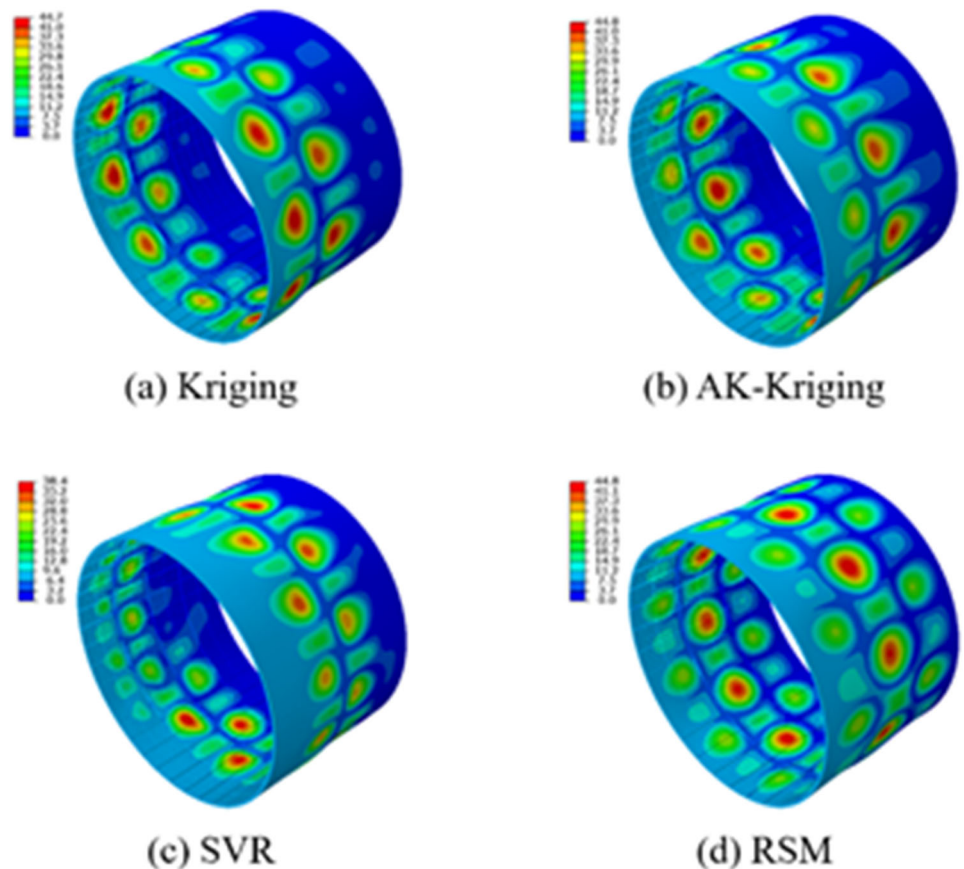
the RSM and SVR show the less relative error for prediction load capacity than the Kriging but the mass is not satisfied the optimum condition using the evaluating optimization model. However, AK-Kriging model is significantly improved the accuracy of predictions for load and mass compared to the RSM and SVR. The Kriging model is provided more accurate result for mass than RSM, while the stochastic term in Kriging model is not improved the accuracy of predicted load compared to the RSM.

Buckling modes at optimum design point for Kriging, AK-Kriging, SVR and RSM models for HSS are compared and displayed in Fig. 7. Similarly, it can be found that, these buckling modes are all global buckling modes

6 Conclusions

In optimization complex engineering problems, the finding optimal design is time consuming process due to applying the finite element analyzer. The accurate optimum result for real engineering problems is vital issue to safe and reliable design conditions. A hybrid statistical and nature-inspired optimization method using active learning-based Kriging method combined by Grey Wolf optimizer (GWO) named AK-GWO is proposed to enhance the accuracy of optimal design condition for the hierarchical stiffened shells (HSS). To enhance the accuracy and efficiency of optimization for HSS for both load capacity as objective and mass as constraint, the active process can be implemented using Kriging model. An active learning process applied in Kriging is proposed using active and adaptive points. Using optimum determined by GWO, the active points are determined from initial simulated data, while the adaptive points are computed using convex procedure for training Kriging model. The accuracy of proposed AK-GWO are compared with several modelling methods as Kriging, support vector regression (SVR) and response surface method (RSM) which, are combined by GWO. The optimization results for maximum load-carrying capacity of HSS indicated that AK-GWO preformed superior accuracy compared to other models. The accuracy of optimum results using AK-GWO is improved about 10%, 6% and 7% for load and about 1%, 4% and 3% for mass compared to Kriging, SVR, and RSM, respectively. The mass constraint based results obtained by RSM and SVR are not satisfied, while the hybrid AK-GWO method is provided the accurate results with safe condition for HSS. The proposed optimization framework can be tested for searching the optimal condition of complex engineering problem, in future.

Compliance with ethical standards

Conflict of interest The authors declare that they have no conflict of interest.

References

1. Singh K, Zhao W, Jrad M, Kapania RK (2019) Hybrid optimization of curvilinearly stiffened shells using parallel processing. J Aircr 56(3):1068–1079. https://doi.org/10.2514/1.c035069
2. Wagner HNR, Hühne C, Niemann S, Tian K, Wang B, Hao P (2018) Robust knockdown factors for the design of cylindrical shells under axial compression: analysis and modeling of stiffened and unstiffened cylinders. Thin-Walled Struct 127:629–645. https://doi.org/10.1016/j.tws.2018.01.041
3. Bagheri M, Jafari AA, Sadeghifar M, Fortin-Simpson J (2016) Comparisons of buckling-to-weight behavior of cylindrical shells with composite and metallic stiffeners. Mech Adv Mater Struct 23(3):353–361. https://doi.org/10.1080/15376494.2014.981611
4. Duc ND, Tuan ND, Tran P, Cong PH, Nguyen PD (2016) Nonlinear stability of eccentrically stiffened S-FGM elliptical cylindrical shells in thermal environment. Thin-Walled Struct 108:280–290. https://doi.org/10.1016/j.tws.2016.08.025
5. Ning X, Pellegrino S (2015) Imperfection-insensitive axially loaded thin cylindrical shells. Int J Solids Struct 62:39–51. https://doi.org/10.1016/j.ijsolstr.2014.12.030
6. Shahgholian-Ghahfarokhi D, Rahimi G (2019) Buckling analysis of composite lattice sandwich shells under uniaxial compression based on the effective analytical equivalent approach. Compos B Eng 174:106932. https://doi.org/10.1016/j.compositesb.2019.106932
7. Shahgholian-Ghahfarokhi D, Rahimi G (2018) Buckling load prediction of grid-stiffened composite cylindrical shells using the vibration correlation technique. Compos Sci Technol 167:470–481. https://doi.org/10.1016/j.compscitech.2018.08.046
8. Wang B, Hao P, Li G, Zhang J-X, Du K-F, Tian K, Wang X-J, Tang X-H (2014) Optimum design of hierarchical stiffened shells for low imperfection sensitivity. Acta Mech Sin 30:391–402. https://doi.org/10.1007/s10409-014-0003-3
9. Wang B, Tian K, Zhou C, Hao P, Zheng Y, Ma Y, Wang J (2017) Grid-pattern optimization framework of novel hierarchical stiffened shells allowing for imperfection sensitivity. Aerosp Sci Technol 62:114–121. https://doi.org/10.1016/j.ast.2016.12.002
10. Zeng M, Zhou H (2018) New target performance approach for a super parametric convex model of non-probabilistic reliability-based design optimization. Comput Methods Appl Mech Eng 339:644–662
11. Wu H, Lai C, Sun F, Li M, Ji B, Wei W, Liu D, Zhang X, Fan H (2018) Carbon fiber reinforced hierarchical orthogrid stiffened cylinder: fabrication and testing. Acta Astronaut 145:268–274. https://doi.org/10.1016/j.actaastro.2018.01.064
12. Tian K, Wang B, Hao P, Waas AM (2018) A high-fidelity approximate model for determining lower-bound buckling loads for stiffened shells. Int J Solids Struct 148:14–23
13. Wang B, Zhu S, Hao P, Bi X, Du K, Chen B, Ma X, Chao YJ (2018) Buckling of quasi-perfect cylindrical shell under axial compression: a combined experimental and numerical investigation. Int J Solids Struct 130:232–247
14. Tian K, Wang B, Zhang K, Zhang J, Hao P, Wu Y (2018) Tailoring the optimal load-carrying efficiency of hierarchical stiffened shells by competitive sampling. Thin-Walled Struct 133:216–225
15. Wang B, Tian K, Zhao H, Hao P, Zhu T, Zhang K, Ma Y (2017) Multilevel optimization framework for hierarchical stiffened

shells accelerated by adaptive equivalent strategy. Appl Compos Mater 24(3):575–592

16. Keshtegar B, Hao P, Wang Y, Hu Q (2018) An adaptive response surface method and Gaussian global-best harmony search algorithm for optimization of aircraft stiffened panels. Appl Soft Comput 66:196–207

17. Hao P, Wang B, Li G, Meng Z, Tian K, Tang X (2014) Hybrid optimization of hierarchical stiffened shells based on smeared stiffener method and finite element method. Thin-Walled Struct 82:46–54

18. Zhao Y, Chen M, Yang F, Zhang L, Fang D (2017) Optimal design of hierarchical grid-stiffened cylindrical shell structures based on linear buckling and nonlinear collapse analyses. Thin-Walled Struct 119:315–323

19. Tian K, Zhang J, Ma X, Li Y, Sun Y, Hao P (2019) Buckling surrogate-based optimization framework for hierarchical stiffened composite shells by enhanced variance reduction method. J Reinf Plast Compos 38(21–22):959–973

20. Tian K, Li Z, Ma X, Zhao H, Zhang J, Wang B (2020) Toward the robust establishment of variable-fidelity surrogate models for hierarchical stiffened shells by two-step adaptive updating approach. Struct Multidisc Optim 61:1515–1528

21. Keshtegar B, Hao P, Wang Y, Li Y (2017) Optimum design of aircraft panels based on adaptive dynamic harmony search. Thin-Walled Struct 118:37–45

22. Gao L, Xiao M, Shao X, Jiang P, Nie L, Qiu H (2012) Analysis of gene expression programming for approximation in engineering design. Struct Multidiscip Optim 46(3):399–413. https://doi.org/10.1007/s00158-012-0767-7

23. Zhang Y, Gao L, Xiao M (2020) Maximizing natural frequencies of inhomogeneous cellular structures by Kriging-assisted multi-scale topology optimization. Comput Struct 230:106197

24. Lu C, Feng Y-W, Fei C-W, Bu S-Q (2020) Improved decomposed-coordinated Kriging modeling strategy for dynamic probabilistic analysis of multicomponent structures. IEEE Trans Reliab 69(2):440–457

25. Li H, Liu T, Wang M, Zhao D, Qiao A, Wang X, Gu J, Li Z, Zhu B (2017) Design optimization of stent and its dilatation balloon using Kriging surrogate model. Biomed Eng Online 16(1):13. https://doi.org/10.1186/s12938-016-0307-6

26. Kolahchi R, Zhu S-P, Keshtegar B, Trung N-T (2020) Dynamic buckling optimization of laminated aircraft conical shells with hybrid nanocomposite martial. Aerosp Sci Technol 98:105656

27. Xiao M, Zhang J, Gao L, Lee S, Eshghi AT (2019) An efficient Kriging-based subset simulation method for hybrid reliability analysis under random and interval variables with small failure probability. Struct Multidiscip Optim 59(6):2077–2092

28. Zhang J, Xiao M, Gao L, Chu S (2019) A combined projection-outline-based active learning Kriging and adaptive importance sampling method for hybrid reliability analysis with small failure probabilities. Comput Methods Appl Mech Eng 344:13–33

29. Zhang J, Xiao M, Gao L, Fu J (2018) A novel projection outline based active learning method and its combination with Kriging metamodel for hybrid reliability analysis with random and interval variables. Comput Methods Appl Mech Eng 341:32–52

30. Seghier MEAB, Keshtegar B, Correia JA, Lesiuk G, De Jesus AM (2019) Reliability analysis based on hybrid algorithm of M5 model tree and Monte Carlo simulation for corroded pipelines: Case of study X60 Steel grade pipes. Eng Fail Anal 97:793–803

31. Sun Z, Wang J, Li R, Tong C (2017) LIF: A new Kriging based learning function and its application to structural reliability analysis. Reliab Eng Syst Saf 157:152–165. https://doi.org/10.1016/j.ress.2016.09.003

32. Keshtegar B, Kisi O (2018) RM5Tree: radial basis M5 model tree for accurate structural reliability analysis. Reliab Eng Syst Saf 180:49–61. https://doi.org/10.1016/j.ress.2018.06.027

33. Fei C-W, Lu C, Liem RP (2019) Decomposed-coordinated surrogate modeling strategy for compound function approximation in a turbine-blisk reliability evaluation. Aerosp Sci Technol 95:105466

34. Xiao M, Zhang J, Gao L (2020) A system active learning Kriging method for system reliability-based design optimization with a multiple response model. Reliab Eng Syst Saf 199:106935. https://doi.org/10.1016/j.ress.2020.106935

35. Zhang J, Gao L, Xiao M (2020) A new hybrid reliability-based design optimization method under random and interval uncertainties. Int J Numer Methods Eng. https://doi.org/10.1002/nme.6440

36. Fei C-W, Li H, Liu H-T, Lu C, Keshtegar B (2020) Multilevel nested reliability-based design optimization with hybrid intelligent regression for operating assembly relationship. Aerosp Sci Technol 103:105906. https://doi.org/10.1016/j.ast.2020.105906

37. Yang X-S (2010) Firefly algorithm, stochastic test functions and design optimisation. arXiv preprint. arXiv:10031409

38. Cai Y, Zhang L, Gu J, Yue Y, Wang Y (2018) Multiple meta-models based design space differentiation method for expensive problems. Struct Multidiscip Optim 57(6):2249–2258. https://doi.org/10.1007/s00158-017-1854-6

39. Keshtegar B, Meng D, Ben Seghier MEA, Xiao M, Trung N-T, Bui DT (2020) A hybrid sufficient performance measure approach to improve robustness and efficiency of reliability-based design optimization. Eng Comput. https://doi.org/10.1007/s00366-019-00907-w

40. Xiao N-C, Yuan K, Zhou C (2020) Adaptive Kriging-based efficient reliability method for structural systems with multiple failure modes and mixed variables. Comput Methods Appl Mech Eng 359:112649

41. Mirjalili S, Mirjalili SM, Lewis A (2014) Grey wolf optimizer. Adv Eng Softw 69:46–61

42. Keshtegar B, Bagheri M, Meng D, Kolahchi R, Trung N-T (2020) Fuzzy reliability analysis of nanocomposite ZnO beams using hybrid analytical-intelligent method. Eng Comput. https://doi.org/10.1007/s00366-020-00965-5

43. Jayakumar N, Subramanian S, Ganesan S, Elanchezhian E (2016) Grey wolf optimization for combined heat and power dispatch with cogeneration systems. Int J Electr Power Energy Syst 74:252–264

44. Krige DG (1951) A statistical approach to some basic mine valuation problems on the Witwatersrand. J South Afr Inst Min Metall 52(6):119–139

45. Heddam S, Keshtegar B, Kisi O (2020) Predicting total dissolved gas concentration on a daily scale using Kriging interpolation, response surface method and artificial neural network: case study of Columbia river Basin Dams, USA. Nat Resour Res 29:1801–1818

46. Sakata S, Ashida F, Zako M (2003) Structural optimization using Kriging approximation. Comput Methods Appl Mech Eng 192(7–8):923–939

47. Huang D, Allen TT, Notz WI, Miller RA (2006) Sequential Kriging optimization using multiple-fidelity evaluations. Struct Multidiscip Optim 32(5):369–382

48. Jiang C, Qiu H, Gao L, Wang D, Yang Z, Chen L (2020) Real-time estimation error-guided active learning Kriging method for time-dependent reliability analysis. Appl Math Model 77:82–98. https://doi.org/10.1016/j.apm.2019.06.035

49. Yun W, Lu Z, Jiang X (2018) An efficient reliability analysis method combining adaptive Kriging and modified importance sampling for small failure probability. Struct Multidiscip Optim 58(4):1383–1393. https://doi.org/10.1007/s00158-018-1975-6

50. Zhang J, Xiao M, Gao L (2019) A new method for reliability analysis of structures with mixed random and convex variables. Appl Math Model 70:206–220

51. Zhang J, Xiao M, Gao L, Chu S (2019) Probability and interval hybrid reliability analysis based on adaptive local approximation of projection outlines using support vector machine. Comput Aided Civ Infrastruct Eng 34(11):991–1009

52. Dubourg V, Sudret B, Bourinet J-M (2011) Reliability-based design optimization using Kriging surrogates and subset simulation. Struct Multidiscip Optim 44(5):673–690

53. Meng Z, Zhang D, Li G, Yu B (2019) An importance learning method for non-probabilistic reliability analysis and optimization. Struct Multidiscip Optim 59(4):1255–1271. https://doi.org/10.1007/s00158-018-2128-7

54. Lu C, Feng Y-W, Liem RP, Fei C-W (2018) Improved Kriging with extremum response surface method for structural dynamic reliability and sensitivity analyses. Aerosp Sci Technol 76:164–175

55. Li Y, Wu Y, Zhao J, Chen L (2017) A Kriging-based constrained global optimization algorithm for expensive black-box functions with infeasible initial points. J Glob Optim 67(1):343–366. https://doi.org/10.1007/s10898-016-0455-z

56. Kowsar R, Keshtegar B, Miyamoto A (2019) Understanding the hidden relations between pro-and anti-inflammatory cytokine genes in bovine oviduct epithelium using a multilayer response surface method. Sci Rep 9(1):1–17